Supplemental Material

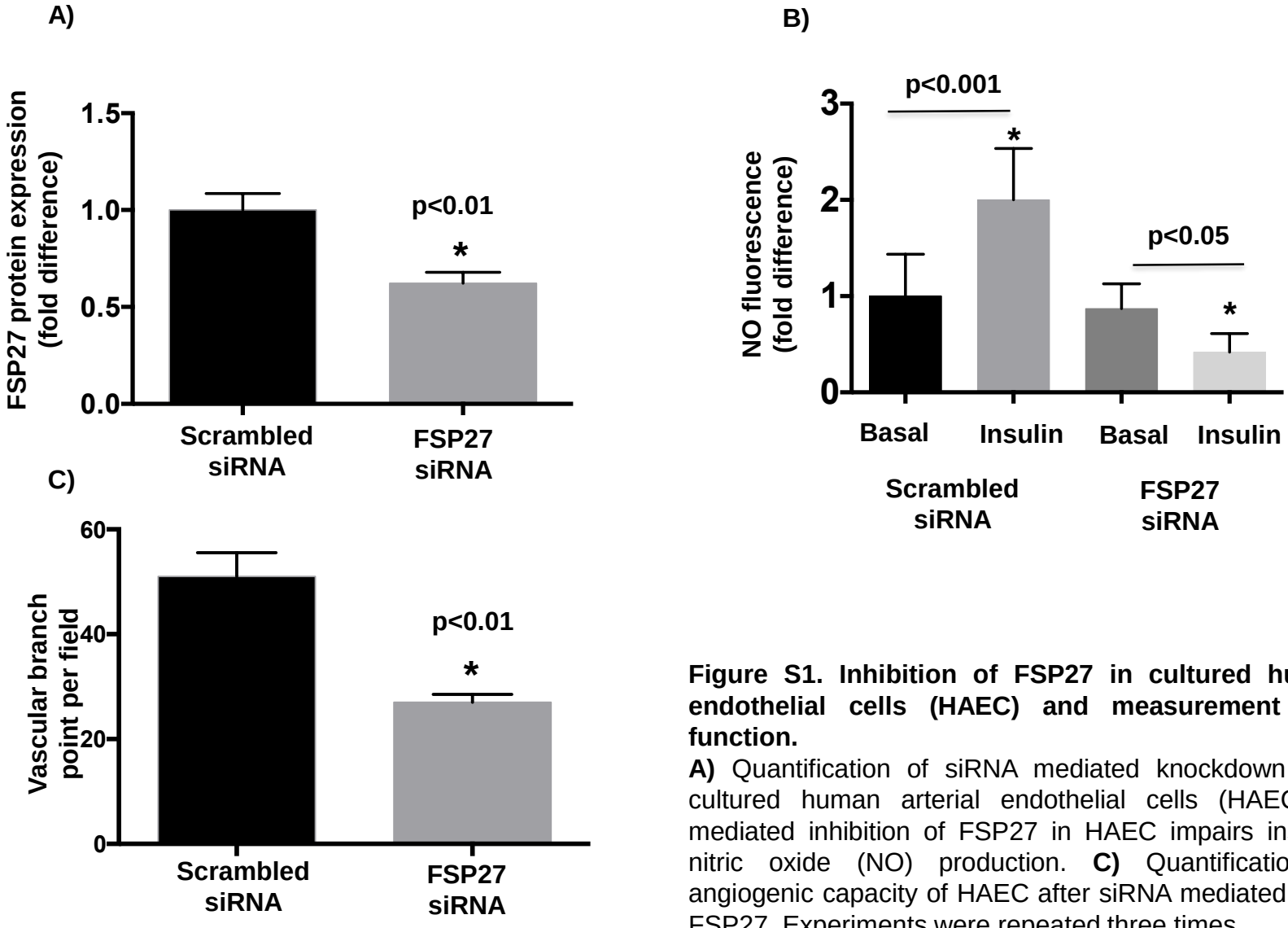

Figure S1. Inhibition of FSP27 in cultured human arterial endothelial cells (HAEC) and measurement of vascular function.

A) Quantification of siRNA mediated knockdown of FSP27 in cultured human arterial endothelial cells (HAEC). **B)** siRNA mediated inhibition of FSP27 in HAEC impairs insulin-mediated nitric oxide (NO) production. **C)** Quantification of in-vitro angiogenic capacity of HAEC after siRNA mediated knockdown of FSP27. Experiments were repeated three times.

Figure S2. Co-localization of VEGF-A and FSP27 in primary endothelial cells isolated from human fat.
A) Merged image of FSP27 and VEGF-A **B)** Image of VEGF-A alone **C)** Image of FSP27 alone . Green = VEGF-A, red = FSP27, blue =Dapi, a nuclear stain.

A) **B)** **C)**

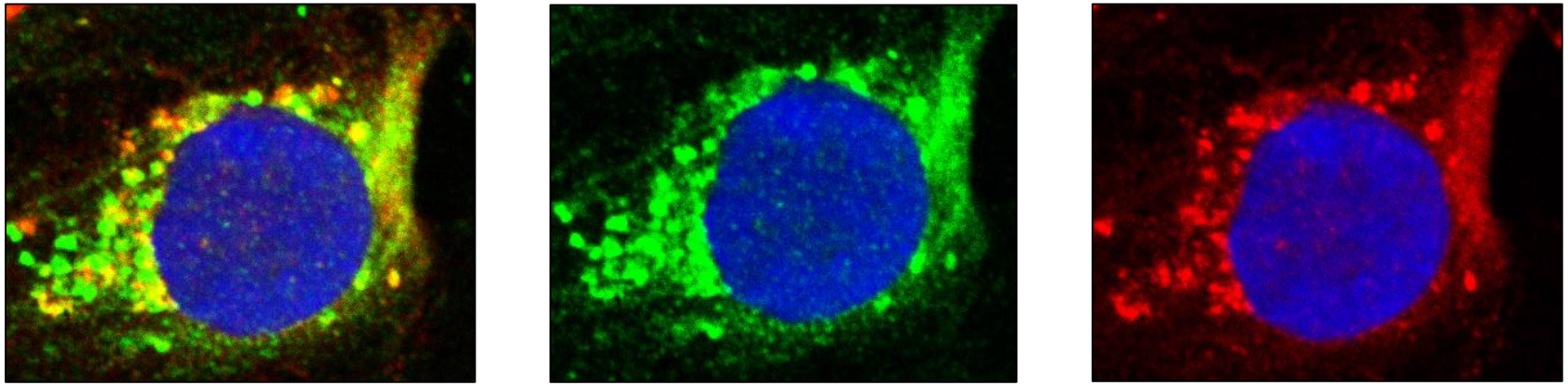

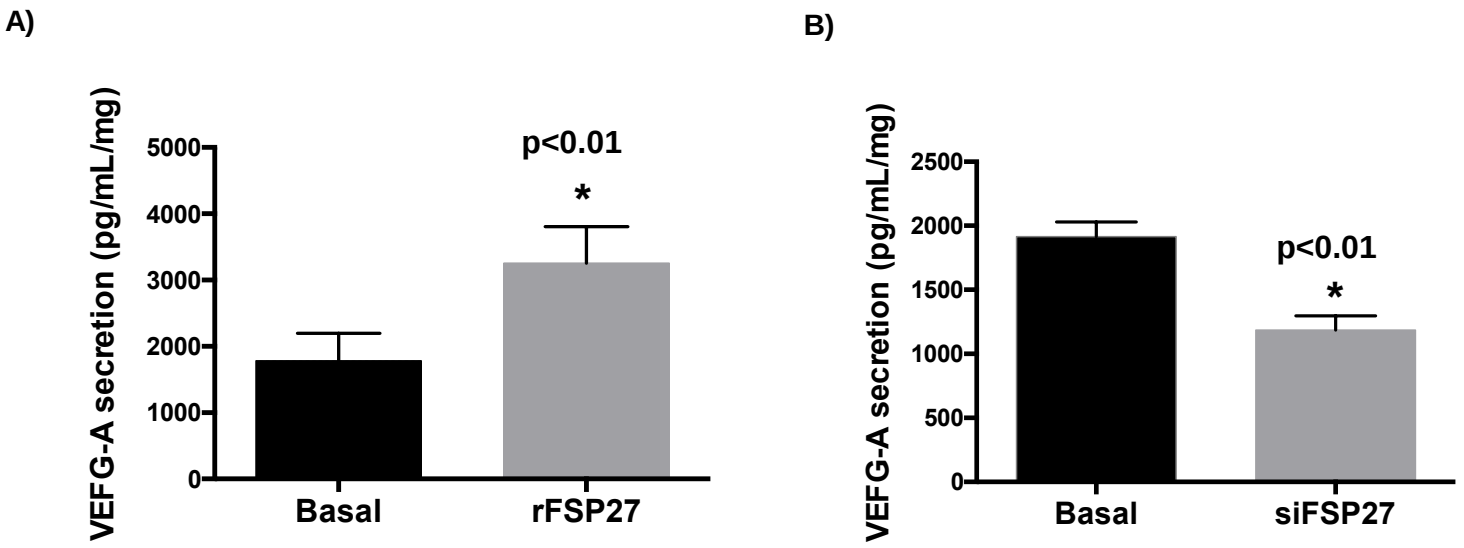

Figure S3. Secretion of VEGF-A from human visceral and subcutaneous fat in response to recombinant human FSP27 and FSP27 siRNA.

A) Exposure of visceral fat to rFSP27 increased VEGF-A secretion (n=11, p<0.01). **B)** Conversely, siRNA FSP27 knockdown significantly decreased VEGF-A secretion from SC fat. (n=10, p<0.01). Data are expressed as picogram (pg) of VEGF-A in mL of media per mg of total protein in tissue.

Figure S4. Protein levels of VEGF-A and FSP27 in human aortic endothelial cells (HAEC) and human peripheral blood macrophages (MACS).

Western blot showing prominent protein expression of FSP27 and VEGF-A in commercially available human aortic endothelial cells (HAEC) while FSP27 expression was essentially absent in MACS.

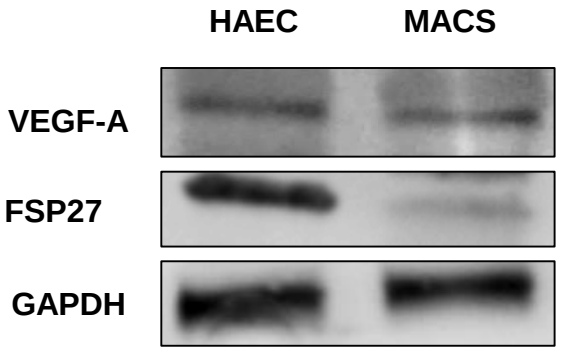

Figure S5. 3-D Immunohistochemistry of fibroblasts demonstrating intracellular/cytosol localization of rFSP27. Green = rFSP27, blue = nucleus.